



Influence of Infill Pattern on Reactive MgO Printed Structures

AlaEddin Douba^(✉), Palash Badjatya, and Shiho Kawashima

Department of Civil Engineering and Engineering Mechanics, Columbia University,
500 West 120th Street, New York, NY 10027, USA
ad3456@columbia.edu

Abstract. The construction industry's increasing interest in additive manufacturing has generated a parallel interest in alternative and supplementary binders. Reactive magnesia (MgO) binders are an attractive and sustainable alternative to Portland cement; they are produced at lower temperatures and can potentially absorb the equivalent amount of CO₂ emitted during production within their service life via carbonation curing. While excessive evaporation in 3D printed Portland cement is usually sought to be prevented, the resulting increase in porosity from the higher surface exposure is a desirable feature for 3D printed MgO that can lead to higher carbon intake. In this work, we utilize nanoclays in combination with methylcellulose as rheological modifiers to produce 25.4 mm MgO paste cylinders with different infill patterns: two open with continuous hollow channels and one solid/closed to mimic a conventionally cast one. Two additional configurations were introduced where the top and bottom layers of the open infills were replaced by a closed layer or a "lid" to conceal the infills' internal structure. The results show that 3D printing of MgO improves compressive strength over cast ones by up to 380% at 28 days of carbonation curing, reaching 40–48 MPa at 1.1 w/b. The results also suggest that infill patterns play a more critical role in stress transfer than carbon intake as finite element analysis confirmed the introduction of localized stresses at the lid layers.

Keywords: Magnesium Oxide · Magnesia · Nanoclays · Sustainability · Carbon sequestration

1 Introduction

Concrete is the second most used material after water and consequently, the manufacture of its most carbon-intensive component, Portland cement, ends up accounting for 7–8% of global CO₂ emissions [1]. Global cement consumption is increasing [2] and so will the associated emissions, unless steps are taken to modify the material to make it less of a carbon emitter or to replace it with alternatives. A viable solution is to use magnesium-based binders that can sequester CO₂ to form relatively stable carbonates that provide adequate strengths for construction under accelerated carbonation conditions [3, 4]. MgO as a material has been used as an additive for various applications but its use as a cement alternative is not as widespread [5, 6]. A non-trivial advantage of MgO is that it can be

mixed with water to form a paste that can be worked with just like conventional cement. More importantly, studies have shown that MgO can absorb CO₂ to form carbonates without the need for elevated temperatures and pressures. Also, MgO can be obtained from non-carbonate sources (e.g. Mg-bearing silicates, industrial wastes, brine) thereby potentially having lower embodied carbon than conventional Portland cement.

Better carbonation and consequently strength gain have been previously achieved through controlling mixture proportions, addition of hydrating agents, and adjusting curing conditions [7, 8]. However, unreacted material remains in the cured systems, potentially limiting further strength gain. 3D printing can help to facilitate carbonation degree as it allows control of geometry to reduce the distance atmospheric CO₂ must travel to reach unreacted MgO, while limiting the amount of material required through topology optimization. Additionally, while excessive evaporation due to the absence of formwork and high surface exposure in 3D printed Portland cement systems is usually sought to be prevented, the resulting increase in porosity can lead to higher carbon intake in MgO systems. There has been relatively modest interest so far in printing using MgO [9] and though results have been promising, the study of the effect of various geometric configurations on strength is limited, which this study aims to address.

2 Materials and Methods

2.1 Materials

The MgO used in this study was obtained from Martin Marietta Magnesia Specialties with the commercial name *MagChem-30*. The MgO was of light-burned type, available as a powder, and its chemical and physical properties are provided in Table 1.

Table 1. Chemical and physical properties of magnesium oxide

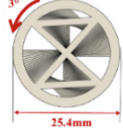
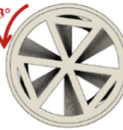

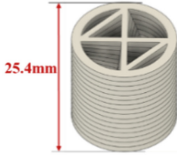


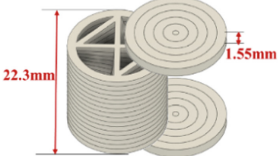

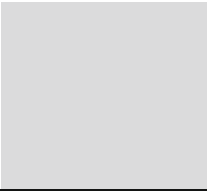
| Chemical composition (%) | | | | | | | Loss on ignition |
|---|-------------------------------|----------------------------------|--------------------------------|--------------------------------|------|-----------------|------------------|
| MgO | CaO | SiO ₂ | Fe ₂ O ₃ | Al ₂ O ₃ | Cl | SO ₃ | (LOI) |
| 98.2 | 0.8 | 0.35 | 0.15 | 0.10 | 0.35 | 0.05 | 1.7% |
| Physical properties | | | | | | | |
| Loose bulk density (g/cm ³) | Median particle size (micron) | Surface area (m ² /g) | Activity index (sec) | % Passing 325 mesh | | | |
| 0.35 | 3-8 | 20-30 | 18 | 99 | | | |

Attapulgite nanoclay (NC) supplied by Active Minerals as *Acti-Gel 208* were used as a thixotropic additive, which have a length of 1.5–2 μm and diameter of 30 nm. To enhance paste cohesion and bleeding resistance, a 14,000 molecular weight methyl cellulose (MC) from Millipore Sigma was also used. This combination of admixtures has been demonstrated to be effective in tailoring the rheology of Portland cement pastes [10]. From static yield stress measurements and printing performance tests, it was found that at 1.1 w/b ratio a dosage of 3 wt. % NC and 1.5 wt. % MC (by addition) was the

lowest satisfactory content, and was the dosage used in this study. The NC was stored as a solution using a magnetic stirrer while MC was added directly in its as-obtained dry powder form.

2.2 Experimental Methodology

Table 2. Various print configurations studied

| | Infill #1 (open) | Infill #2 (open) | Infill #3 (closed) |
|---------------------------|---|---|---|
| Cross-section |  |  |  |
| Uncapped (exposed infill) |  |  |  |
| Capped (hidden infill) |  |  |  |

A syringe table-top printer was used to 3D print MgO cylinders 25.4 mm height and diameter with three infill patterns, as shown in Table 2. Additional cylinders were prepared for infills #1 and #2 where the top and bottom layers were replaced with closed ones to mimic capping, hiding away the internal open infill structure. In addition, cast specimens with conventional molds were prepared and tested for comparison.

To minimize evaporation loss during the first 24 h, the printed specimens were loosely covered with a plastic sheet after printing while ensuring that the sheet did not touch and disturb the specimens. The control specimens were cast in cylindrical molds and covered with a plastic sheet. After 24 h in ambient lab conditions, the samples were transferred to an incubator maintained at 25 °C, 80 ± 5% RH and 20% CO₂ to be carbonated. Compressive strength tests were carried out at the end of 28 days of incubation on an MTS Criterion C43 Electromechanical Testing Machine at a loading rate of 1.27 mm/min. The top and bottom surfaces of all specimens were covered with gypsum paste caps to ensure uniform loading. At least 3 specimens per batch were used to calculate the final average.

2.3 Finite Element Modeling

Finite element analysis (FEA) of all tested specimens was carried out using Autodesk Fusion 360 to investigate the effect of infill patterns and capping on stress transfer. Parabolic tetrahedral elements with 10 nodes were used for meshing. To avoid stress concentration from localized change in curvature, all edges were smoothed with circular parabolic with 0.25 mm radius. Up to 6 refinement steps were carried out per model to reach a convergence tolerance of 5%. The total number of elements used varied between 427,528–865,803. The elastic modulus of MgO was assumed to be 68 GPa with a Poisson's ratio of 0.19 [11]. Boundary conditions were set to fix the bottom and apply a uniform 1 MPa stress at the top, and maximum Von Mises tensile stresses were extracted as an indicator of stress transfer efficiency.

3 Results and Discussions

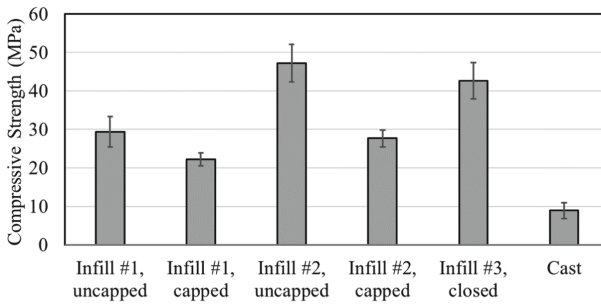


Fig. 1. Aggregated compressive strength results for all batches cured for 28 days in accelerated CO₂ conditions

The results of compressive strength after 28-days of carbonation curing are presented in Fig. 1. It is apparent that all of the 3D printed specimens show a higher strength than the cast control. Infill #3 specimens exceeded the strength of cast specimens by 380%, where the former had an average strength of 42.6 ± 4.7 MPa and the latter had a strength of 8.9 ± 2 MPa. The open infill printed specimens also exceeded the strength of the cast specimens by a significant margin. Between the two open infills, uncapped infill #2 had a higher average strength than that of uncapped infill #1: 47.2 ± 4.9 MPa vs 22.2 ± 1.7 MPa at 28 days, respectively. Uncapped infill #2 was within the margin of error of infill #3 at 28 days. Capping of infill #1 and infill #2 reduced strength by 24% and 42%, respectively. Results indicate that capping does not lead to any positive impact on strength and was in fact detrimental to the strength of specimens.

These results provide preliminary insight into the effects of infill pattern on structural strength. 3D printing clearly has an advantage over conventional casting when using MgO cement. A possible reason for this behavior was speculated as higher porosity in the 3D printed material in the work of Khalil et al. [9]. A higher porosity, due to the lack of protective casing molds, can lead to higher diffusion of CO₂, more carbonation,

and thus higher strength. Another reason for the differences in strength could be the influence of specimen geometry on localized stresses, discussed below.

Table 3. FEA results for compression under 1 MPa

| | Infill #1 | | Infill #2 | | Infill #3 | Cast |
|---------------------------|-----------|--------|-----------|--------|-----------|--------|
| | Uncapped | Capped | Uncapped | Capped | | |
| Volume (mm ³) | 5729 | 6976 | 6267 | 7523 | 9407 | 10756 |
| Number of elements | 581064 | 658530 | 865803 | 735517 | 427528 | 680671 |
| Max tension (MPa) | 2.50 | 15.27 | 2.73 | 10.67 | 2.71 | 2.86 |

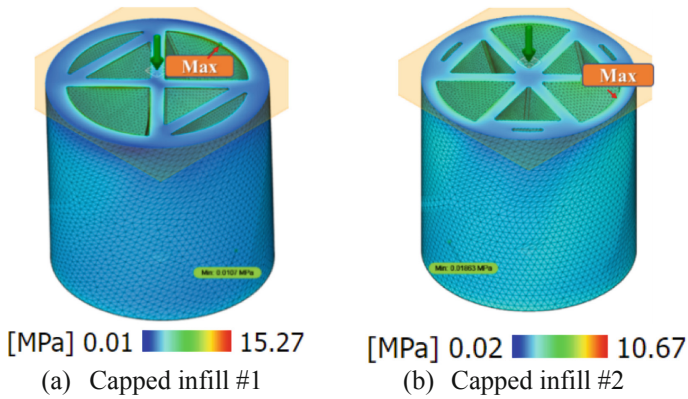


Fig. 2. FEA showing localized stress concentrations at the transfer layer between the cap and internal structure (sliced view).

To further understand the differences in compressive strength of tested configurations, FEA was carried out and the results are summarized in Table 3. Uncapped infills #1 and #2, infill #3, and cast show similar stress concentration levels corresponding to the 1 MPa load applied in the model. Therefore, the differences in strength observed in 3D printed specimens versus cast ones can be attributed to improved carbonation. The differences between infills #1, #2 and #3 can be correlated to differences in the amount of material present rather than stress transfer where infills #1 and #2 represent 39% and 33% reduction in volume, respectively. Capping introduced significant localized stress concentrations between the cap and the internal structure, as shown in Fig. 2, which partially explains the decrease in strength discussed earlier.

4 Conclusion

In this work, we showed that 3D printed MgO, achieved by utilizing a mixture of nanoclays and methyl cellulose rheological modifiers, is a promising material that can reach

compressive strengths of 50 MPa. The increase in strength of 3D printed parts compared to cast ones was mainly attributed to increased porosity resulting from higher water evaporation, which, in turn, facilitated CO₂ penetration. Finally, FEA results support that the density of the infill pattern has greater influence on compressive strength if no abrupt changes occur in the structure, where stress concentrations resulted from the abrupt introduction of the capping layers.

Acknowledgments. The authors would like to acknowledge the National Science Foundation (Award #1653419) and Columbia University's School of Engineering and Applied Science (SEAS) Interdisciplinary Research Seed (SIRS) Program for financial support.

References

1. Andrew, R.M.: Global CO₂ emissions from cement production. *Earth Syst. Sci. Data* **10**(1), 195–217 (2018). <https://doi.org/10.5194/essd-10-195-2018>
2. IEA: Technology Roadmap - Low-Carbon Transition in the Cement Industry, Paris (2018). <https://www.iea.org/reports/technology-roadmap-low-carbon-transition-in-the-cement-industry>
3. Al-Tabbaa, A.: Reactive magnesia cement. In: *Eco-Efficient Concrete*, pp. 523–543. Elsevier (2013)
4. Harrison, A.J.W.: Reactive magnesium oxide cements. U.S. Patent No. 7,347,896 (2008)
5. Du, C.: A review of magnesium oxide in concrete. *Concr. Int.* **27**(12), 45–50 (2005)
6. Walling, S.A., Provis, J.L.: Magnesia-based cements: a journey of 150 years, and cements for the future? *Chem. Rev.* **116**(7), 4170–4204 (2016). <https://doi.org/10.1021/acs.chemrev.5b00463>
7. Ma, S., Akca, A.H., Esposito, D., Kawashima, S.: Influence of aqueous carbonate species on hydration and carbonation of reactive MgO cement. *J. CO₂ Utilization* **41**, 101260 (2020). <https://doi.org/10.1016/j.jcou.2020.101260>
8. Unluer, C., Al-Tabbaa, A.: Enhancing the carbonation of MgO cement porous blocks through improved curing conditions. *Cem. Concr. Res.* **59**, 55–65 (2014). <https://doi.org/10.1016/j.cemconres.2014.02.005>
9. Khalil, A., Wang, X., Celik, K.: 3D printable magnesium oxide concrete: towards sustainable modern architecture. *Addit. Manuf.* **33**, 101145 (2020). <https://doi.org/10.1016/j.addma.2020.101145>
10. Douba, A., Kawashima, S.: Use of nanoclays and methylcellulose to tailor rheology for three-dimensional concrete printing. *ACI Mater. J.* **118**(6), 275–289 (2021)
11. Pereira, A.H.A., Venet, M., Tonnesen, T., Rodrigues, J.A.: Development of equipment for non-destructive characterization of elastic moduli of ceramic materials. *Ceramica* **56**(338), 118–122 (2010)